AIAA JOURNAL
Vol. 33, No. 2, February 1995

Similarity Rule for Jet-Temperature Effects on Transonic Base Pressure

Keisuke Asai*
National Aerospace Laboratory, Tokyo 182, Japan

On the basis of the similarity rule for jet interaction, a hot jet can be simulated in a cryogenic wind tunnel with a test gas at ambient or moderately elevated temperatures. By using this approach, jet-temperature effects on the base pressure of a cylindrical afterbody model at transonic speeds have been investigated in the 0.1-m transonic cryogenic wind tunnel at the National Aerospace Laboratory. Mixtures of nitrogen and either methane, argon, or helium at varying temperatures were used as a jet gas to determine separate effects of jet temperature, specific heat ratio, and gas constant. It has been found that data obtained for various jet conditions can be correlated very well with two similarity parameters: the plume maximum diameter for the plume shape effect and the jet to freestream mass flux ratio for the jet entrainment effect. To verify this similarity rule, the same model was tested in an ambient wind tunnel. It was found that an ambient temperature gas having low molecular weight could simulate the jet temperature effects on the transonic base pressure.

Nomenclature

A_e/A^* = nozzle exit area to nozzle throat area ratio
C_p = specific heat at constant pressure, J/kg-K
C_v = specific heat at constant volume, J/kg-K
C_{pb} = base pressure coefficient, $(p_b - p_0)/q$
d_1/d_e = ratio of maximum plume diameter to nozzle exit diameter
M = Mach number
NPR = nozzle pressure ratio, p_{tj}/p_0
p = pressure, kPa
q = dynamic pressure, kPa
R = gas constant, J/kg-K
T = temperature, K
V = velocity, m/s
γ = ratio of specific heats, C_p/C_v
ρ = density, kg/m³

Subscripts

0 = freestream
b = base
j = jet flow
t = stagnation

Introduction

SINCE the beginning of the jet age, a realistic simulation of jet engine exhaust has been one of the major concerns among wind-tunnel engineers. Actual combustion gas exhausted from a turbojet engine is as hot as 1000 K or higher at afterburning condition. However, jet-temperature effects are usually ignored, and tests are mostly performed using compressed cold air to represent a hot jet exhaust.

The effects of jet temperature are known to be very important in some critical aerodynamic problems such as the nozzle afterbody drag at transonic speeds. It was reported in Ref. 1 that a large reduction in afterbody drag with reheat was found in flight testing of the Tornado aircraft. It was also reported in Ref. 2 that the flight value of the base pressure on the solid rocket booster of the Space Shuttle was found to be much higher than predicted in cold jet tests. These observations in flight are believed to be attributed to the effects of jet temperature on afterbody flow.

Received April 28, 1994; presented as Paper 94-2571 at the AIAA 18th Aerospace Ground Testing Conference, Colorado Springs, CO, June 20–23, 1994; revision received Oct. 3, 1994; accepted for publication Oct. 15, 1994.

*Senior Researcher, Aircraft Aerodynamics Division. Member AIAA.

As summarized in Ref. 1, extensive experimental investigations have been performed on jet-temperature effects on the afterbody drag by using hydrogen-peroxide decomposition and ethylene/air burning. From these previous studies,[3,4] it has been found that there are two distinguishable features about the jet-temperature effects on afterbody flow (Fig. 1).

First, a jet exhaust behaves like a solid body and blocks the external flow during its expansion to freestream pressure. This effect, referred to as the plume shape effect, is correlated very well with parameters such as the initial jet expansion angle[3] or the maximum plume diameter to nozzle exit diameter ratio.[4] These correlation parameters are a function of not only the nozzle pressure ratio p_{tj}/p_0 but also the specific heat ratio of the jet gas γ_j.

For an attached afterbody, the plume shape effect accounts for most of the observed effect of jet temperature. For a separated afterbody, however, the plume shape effect is only part of the story and the additional effect due to jet entrainment through the turbulent mixing is significant. The entrainment effect is more difficult to evaluate than the plume shape effect since various flow properties such as temperature, velocity, and density are involved in the entrainment process.

Peters[5] of the Arnold Engineering Development Center found from his experiment using cold N_2/H_2 mixtures that the variation in gas constant has an effect similar to that caused by jet temperature variation. From this result, he has inferred that the product of R and T should relate entrainment effects. To the author's knowledge, however, this hypothesis has not been verified to date.

As a solution to this frustrating problem, the author used a novel hot-jet simulation technique that utilizes the advantage of a cryogenic wind tunnel in flow simulation.[6–8] Since the working gas of a cryogenic wind tunnel is as cold as 100 K, a hot jet can be simulated with a jet gas at ambient or moderately elevated temperatures. This

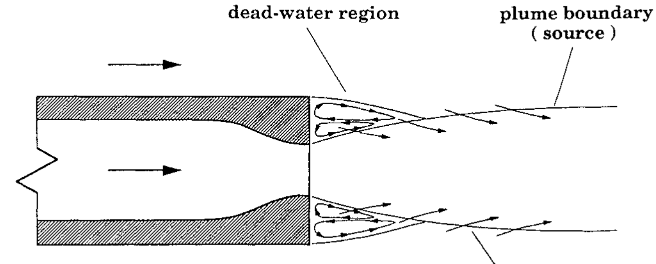

Fig. 1 Schematic model of jet interaction with afterbody flow.

greatly relieves the requirements for model construction and instrumentation. In addition, complete simulation of afterburning turbojet exhausts can be easily achieved by using a nitrogen-methane mixture at moderately elevated temperature as a jet gas.

By utilizing such unique capabilities of the cryogenic wind tunnel, the similarity rule for jet temperature effects on the base pressure of a cylindrical blunt-based afterbody model has been investigated in the present study. Tests were conducted in the 0.1-m transonic cryogenic wind tunnel at the National Aerospace Laboratory (NAL) using different gas mixtures of nitrogen and either methane, argon, or helium at varying temperatures as a jet gas. This allowed the tests to cover a wide range of the jet temperature ratio T_{tj}/T_{t0}, the gas constant R_j, and the specific heat ratio γ_j.

In this report, the details of the present experiment are described and the obtained results are discussed with an emphasis on determining the similarity parameters governing the plume shape effect and the jet entrainment effect on transonic base pressure.

Description of Experiment

Test Facility

The present study was conducted in two small facilities at NAL: the NAL 0.1-m transonic cryogenic wind tunnel (0.1-m TCWT) and the NAL 0.18-m transonic atmospheric wind tunnel (0.18-m TAWT).

The 0.1-m TCWT[9] is a closed-circuit, fan-driven wind tunnel operated with cryogenic nitrogen as the working gas. At transonic speeds, stagnation temperature can be varied from 90 to 150 K with the maximum stagnation pressure up to 200 kPa. The test section is 0.1-m square and equipped with slotted top and bottom walls of 4% porosity and solid sidewalls. On the other hand, the 0.18-m TAWT[10] is a closed-circuit fan-driven wind tunnel operated at atmospheric conditions. The test section is 0.18-m square and incorporates 20% porosity perforated top and bottom walls and solid sidewalls. The 0.18-m TAWT tests were performed to verify the results obtained from the 0.1-m TCWT tests.

Model

A cylindrical blunt-based nozzle afterbody model was used as a test article. This model had an overall length of 140 mm and a model diameter of 10 mm, and it incorporated a 18.9-deg cone-cylinder nose. The details of the nozzle and afterbody contour are illustrated in Fig. 2. The exit diameter of the convergent nozzle was 3.5 mm. In both the 0.1-m TCWT and the 0.18-m TAWT, the model was strut mounted in the test section at zero angle of attack. A jet gas was supplied from outside through insulated piping.

One pressure tap and one thermocouple were provided in the model base area, and one wall pressure tap was incorporated 3 model diameters upstream of the base to measure the freestream reference pressure. As reported in Ref. 11, the upstream influence of the base is negligible at this location. Using the reference Mach number instead of the plenum Mach number allows a correction for the effects of the model blockage, which is as large as 3.0% in the 0.1-m TCWT. Inside the model, a pitot tube and a thermocouple were provided to measure the stagnation properties of the jet gas. From these measurements, the internal reference values at the nozzle exit were evaluated by using isentropic relationships.

Gas Supply System

Figure 3 is a schematic diagram of the jet gas supply system. This system consists of gas-blending, pressure-regulating, and temperature-conditioning sections. The gas-blending section is based on a pair of thermal mass flowmeters, both of which were calibrated by using a sonic venturi flowmeter as a reference. The mole fraction of a component gas in the mixture can be varied from 0 to 100% by controlling a flow valve located in one of the gas lines. The temperature of the jet gas was controlled by using either

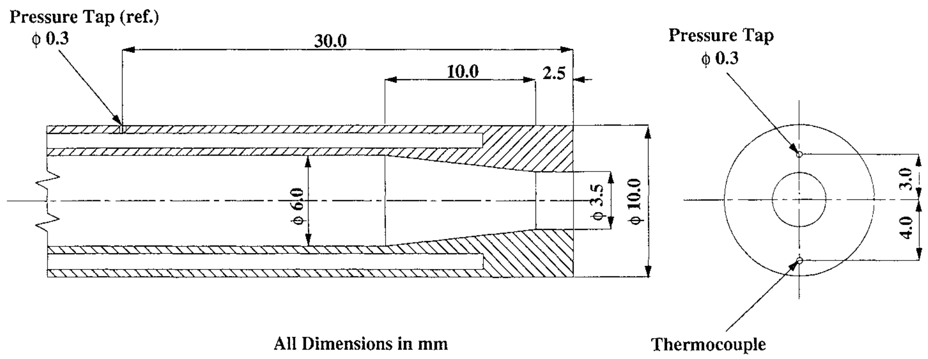

Fig. 2 Details of model afterbody configuration.

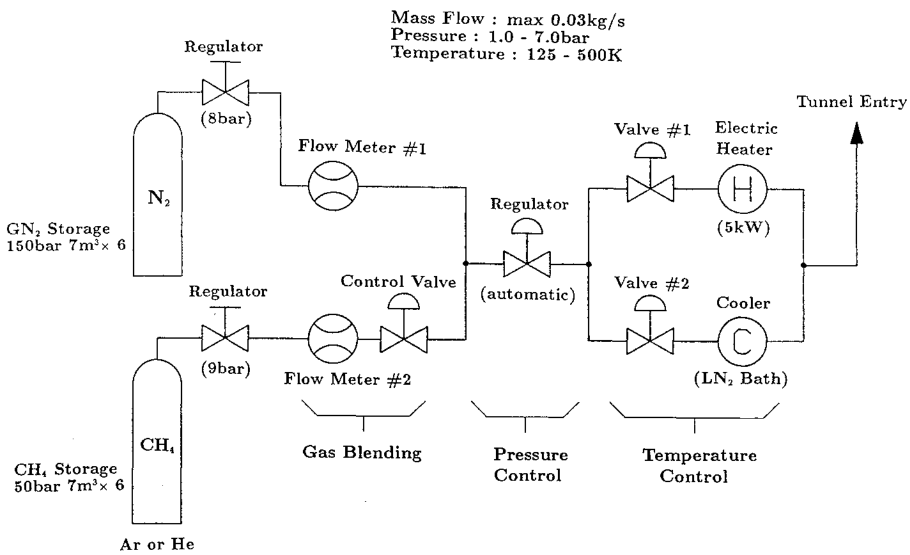

Fig. 3 Schematic diagram of jet gas supply system.

Table 1 Test cases in the 0.1-m TCWT and the 0.18-m TAWT

	Freestream condition				Jet-flow condition				
Facility	Gas	M_0	P_{t0}, kPa	T_{t0}, K	Gas, mole	NPR	T_{tj}/T_{t0}	R_j, J/kg-K	γ_j
0.1-m TCWT	N_2	0.814	110	100	N_2	off–6.0	3.6	297	1.40
0.1-m TCWT	N_2	0.814	110	140	N_2	off–6.0	1.0–3.0	297	1.40
0.1-m TCWT	N_2	0.814	110	140	N_2/CH_4 (0–60%)	off–6.0	2.14–2.86	297–399	1.30–1.40
0.1-m TCWT	N_2	0.814	110	140	N_2/Ar (0–60%)	off–6.0	1.43–2.86	236–297	1.40–1.53
0.1-m TCWT	N_2	0.814	110	140	N_2/He (0–60%)	off–6.0	1.43–2.86	297–611	1.40–1.53
0.18-m TAWT	Air	0.814	Ambient	Ambient	N_2/He (0–100%)	off–8.0	0.96	297–2077	1.40–1.66

an electric heater or an LN_2 bath depending on a set value of T_{tj}. An estimated accuracy in the mole fraction, pressure, and temperature is 5%, 0.5 kPa, and 5 K, respectively.

Test Conditions

Table 1 summarizes test cases conducted in the 0.1-m TCWT and the 0.18-m TAWT. In both tunnels, tests were performed at the same reference freestream Mach number (0.814).

In the 0.1-m TCWT tests, the tunnel stagnation temperature was set at 100 or 140 K, whereas the jet temperature ranged from 125 to 400 K. Mixtures of nitrogen and either methane, argon, or helium were used as a jet gas. This allowed the tests to cover ranges of T_{tj}/T_{t0} from 1.0 to 3.6, R_j from 236 to 611 J/kg-K, and γ_j from 1.30 to 1.53.

On the other hand, the 0.18-m TAWT tests were conducted at atmospheric freestream conditions. Differing mixtures of nitrogen and helium at ambient temperature were used as a jet gas. The jet temperature ratio was maintained at approximately 0.96, whereas R_j and γ_j were varied from 297 to 2077 J/kg-K and from 1.40 to 1.66, respectively.

Results and Discussion

Comparison of Data Obtained at Cryogenic and Ambient Temperatures

Figure 4 shows a comparison of the base pressure data obtained in the 0.1-m TCWT and the 0.18-m TAWT, for the case of T_{tj}/T_{t0} at about 1.0 (corresponding to "cold-jet" condition). As is seen in Fig. 4, the data from the cryogenic method are similar to those from the conventional method for an identical value of jet temperature ratio. This result confirms that the absolute temperature is not important from the viewpoint of jet-flow simulation.

Effect of Jet-Temperature Ratio

Within the temperature range shown in Table 1, a variation in jet temperature alone does not affect either the specific heat ratio or the gas constant. Therefore, it is easy with the cryogenic method to isolate the effect of jet temperature ratio from those of γ_j and R_j.

Figure 5 shows the effect of jet temperature ratio on the base pressure for a nitrogen jet. The same data are plotted in Fig. 6 as a function of the square root of T_{tj}/T_{t0} for various constant NPR. As shown, the base pressure increases with increasing jet-temperature ratio. The variation in C_{pb} for a constant NPR appears to be a linear function of the square root of T_{tj}/T_{t0}. It should be noted here that this increase in C_{pb} results from a pure entrainment effect because the plume shape effect is identical for equal NPR and γ_j. This means that the mass entrainment effect of a jet decreases as jet temperature increases.

Effects of R and T on Jet Entrainment

Argon and helium have the same specific heat ratio (1.66), whereas the molecular weight of Ar (39.9) is larger by an order of magnitude than that of He (4.0). Therefore, mixing either argon or helium with a nitrogen-based jet allows variation in gas constant while maintaining constant γ_j.

In Fig. 7, the variation in C_{pb} for N_2/Ar or N_2/He mixtures is presented for mole ratio of 50%. A value of the specific heat ratio is 1.50 for both the mixtures. The jet temperature was varied from 200 to 400 K, which corresponds to a T_{tj}/T_{t0} variation from 1.43 to 2.88. As shown, the base pressure for the N_2/He mixture is higher than that for the N_2/Ar mixture. It is noted here that an increase in either R_j or T_{tj} causes a rise in base pressure. The same data shown in Fig. 7 are plotted in Fig. 8 against the square root of the product of jet temperature and gas constant. It is seen that an identical change in C_{pb} occurs as a result of varying either R_j or T_{tj}. This is also the case for mole ratio of 25% (γ_j = 1.44). It can be concluded from these results that jet entrainment is a function of the product of gas constant and temperature. This provides a direct experimental evidence to the inference made by Peters[5] on the jet entrainment effect.

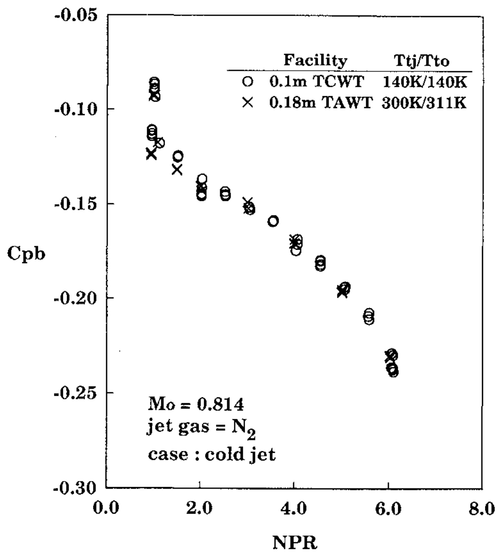

Fig. 4 Comparison of the data obtained in cryogenic and ambient wind tunnels (cold-jet case).

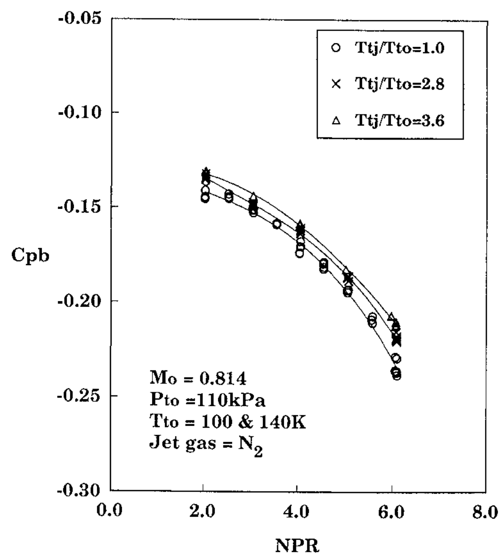

Fig. 5 Effect of jet temperature ratio on C_{pb}.

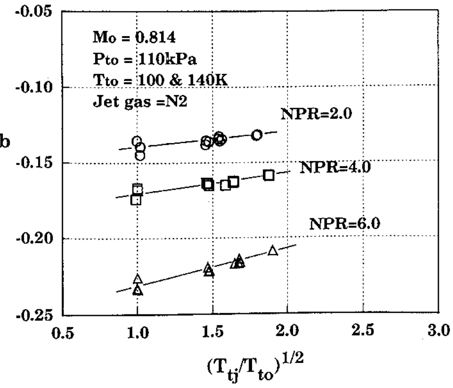

Fig. 6 C_{pb} variation plotted as a function of T_{tj}/T_{t0} (nitrogen jet).

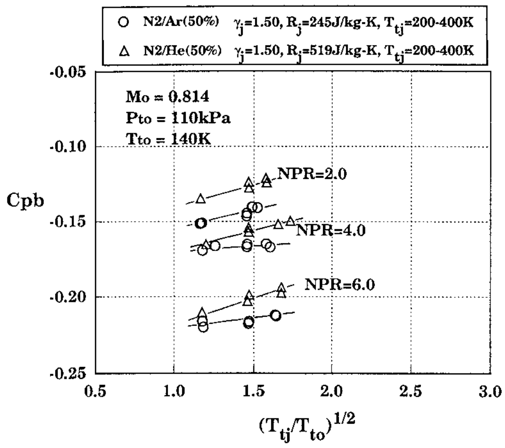

Fig. 7 Effect of gas constant on C_{pb} (mole fraction = 50%).

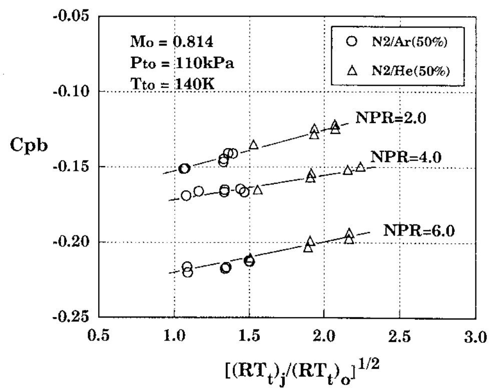

Fig. 8 C_{pb} variation plotted as a function of RT (mole fraction = 50%).

Evaluation of the Similarity Parameters

Table 2 summarizes the relationship between various jet-flow properties. Of these properties, the temperature T and the momentum flux ρV^2 are not suitable to correlate the effect of jet entrainment since neither is a function of the product of R and T.

There still are a number of candidates for a correlation parameter for the jet entrainment effect: density, velocity, mass flux, internal energy, and enthalpy, all of which are a function of the product of R and T.

To identify the parameter essential to the jet entrainment effect, the data need to be plotted for constant values of the plume shape parameter. As previously stated, the plume shape effect is dependent on both NPR and γ_j. Referring to Peters,[4,5] we introduce here the maximum plume diameter to nozzle exit diameter ratio, d_1/d_e, as a correlation parameter for the plume shape effect.

Table 2 Relationship between the basic jet-flow properties

Flow property	p	M	γ	R	T
Temperature, T	—	—	—	—	T
Density, ρ	p	—	—	R^{-1}	T^{-1}
Velocity, V	—	M	$\gamma^{0.5}$	$R^{0.5}$	$T^{0.5}$
Mass flux, ρV	p	M	$\gamma^{0.5}$	$R^{-0.5}$	$T^{-0.5}$
Momentum flux, ρV^2	p	M^2	γ	—	—
Internal energy, $C_v T$	—	—	$1/(\gamma-1)$	R	T
Enthalpy, $C_p T$	—	—	$\gamma/(\gamma-1)$	R	T

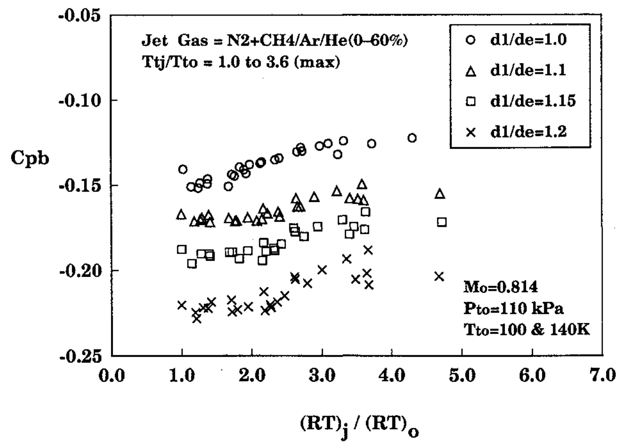

Fig. 9 Correlation of data with d_1/d_e and RT ratio.

From the formula for quasi-one-dimensional isentropic flow, d_1/d_e can be expressed as follows:

$$\frac{d_1}{d_e} = \sqrt{\left[\left(\frac{\gamma_j+1}{2}\right)^{-n} \cdot \left(1+\frac{\gamma_j-1}{2}M_1^2\right)^{n}\right] / M_1(A_e/A^*)} \quad (1)$$

where

$$n = \frac{\gamma_j+1}{2(\gamma_j-1)} \quad (2)$$

and

$$M_1 = \sqrt{\frac{2}{\gamma_j-1}\left(NPR^{(\gamma_j-1)/\gamma_j}-1\right)} \quad (3)$$

A_e/A^* in this case is equal to 1 (convergent nozzle), and M_1 is the isentropically expanded jet Mach number. A value of d_1/d_e is calculated from measurements of NPR and γ_j.

Figures 9–14 represent plots of C_{pb} data for constant d_1/d_e against the RT ratio, the density ratio, the velocity ratio, the mass flux ratio, the internal energy ratio, and the enthalpy ratio, respectively. A comparison of these figures clearly indicates that the mass flux ratio, $(\rho V)_j/(\rho V)_0$, and the internal energy ratio, $(C_v T)_j/(C_v T)_0$, are the most suitable correlation parameters for the jet entrainment effect. The other parameters such as velocity ratio and density ratio are less suitable since there remains considerable scatter of the data at higher values of d_1/d_e.

It should be noted here that the mass flux ratio and the internal energy ratio are not independent of each other. The d_1/d_e, ρV ratio, and $C_v T$ ratio are interrelated through the isentropic flow relationship. In terms of correlating the effects of jet entrainment, the mass flux ratio and the internal energy ratio are equivalent.

From the physical point of view, the mass flux ratio is directly related to the mixing characteristics of shear layers between the jet flow and the external flow. The correlation shown in Fig. 12 can be interpreted as the jet pump effect reducing as the jet mass flux decreases. Mass flux of a jet is reduced with increasing temperature. As shown in Fig. 12, the effect of d_1/d_e becomes small as the mass flux ratio gets smaller. This means that, for a hot jet, the base pressure is mostly affected by the jet entrainment. A net effect due to jet temperature elevation resulted in an increase in the base pressure

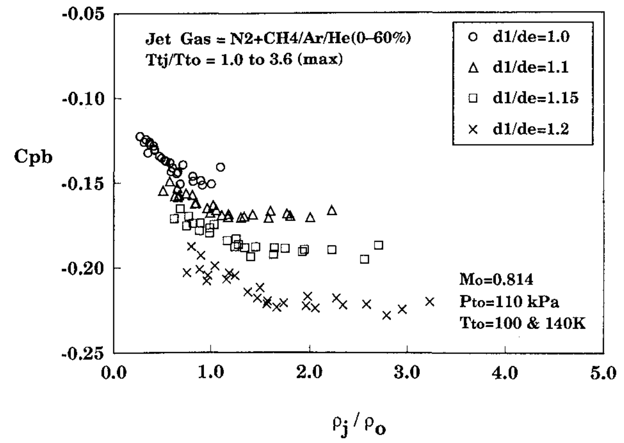

Fig. 10 Correlation of data with d_1/d_e and ρ ratio.

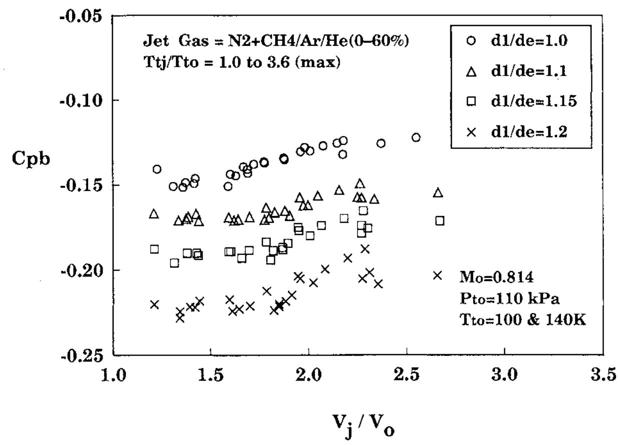

Fig. 11 Correlation of data with d_1/d_e and V ratio.

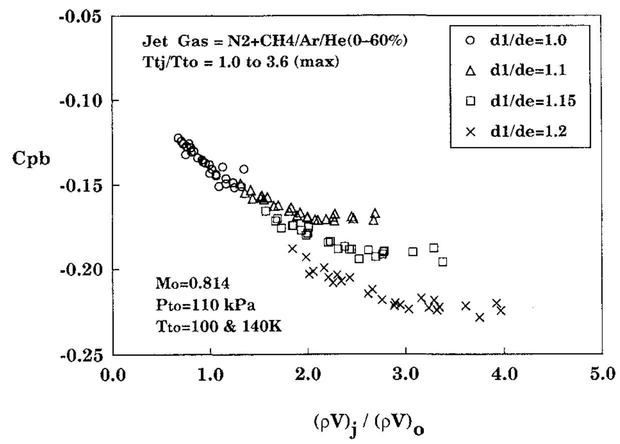

Fig. 12 Correlation of data with d_1/d_e and ρV ratio.

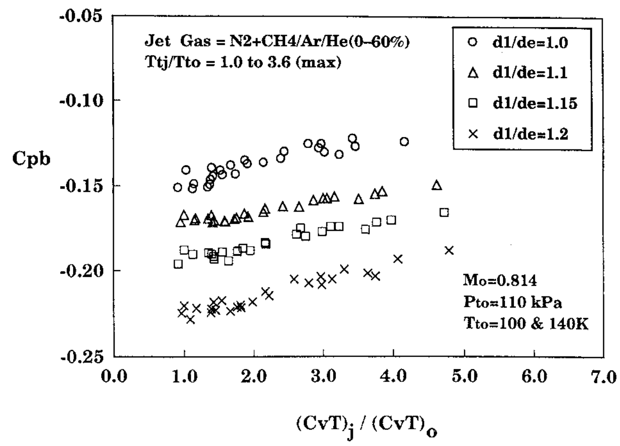

Fig. 13 Correlation of data with d_1/d_e and C_vT ratio.

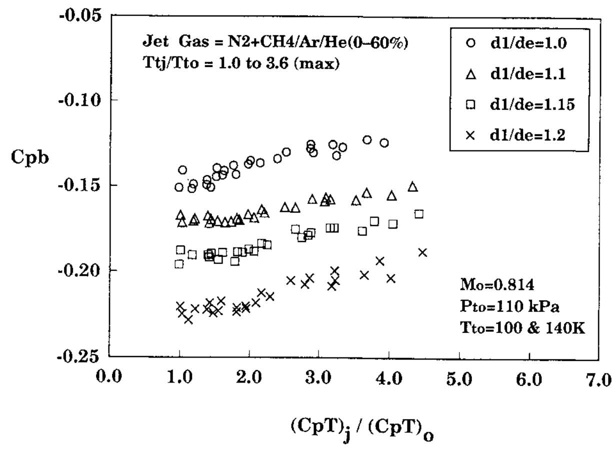

Fig. 14 Correlation of data with d_1/d_e and C_pT ratio.

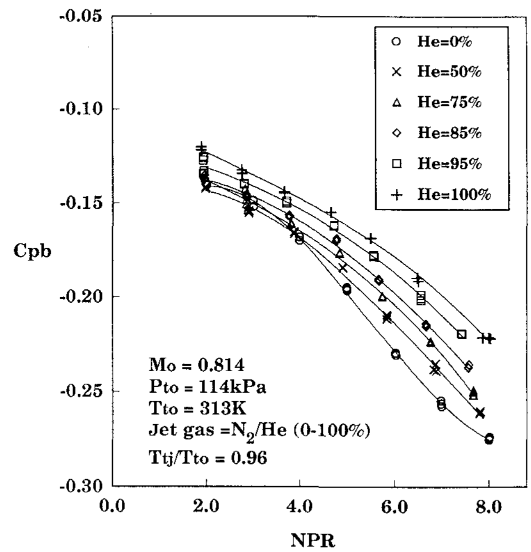

Fig. 15 Effect of mole fraction of helium on C_{pb}.

(reduction in the base drag). It should be remembered here that this result agrees with the experiences in flight of the Tornado and Space Shuttle vehicles.

Simulation of Jet-Temperature Effect Using Low-Molecular-Weight Cold Jet

The similarity rule derived from the cryogenic experiment indicates that, for correct simulation of jet temperature effects, it is not necessary to match the actual values of jet temperature ratio, γ_j, and NPR, but instead the d_1/d_e and ρV ratio should be matched. This suggests that, by using a cold gas having low molecular weight, the effect of jet temperature can be simulated.

To validate this methodology, the same model was tested in the 0.18-m TAWT by using ambient temperature N_2/He mixtures of varying mole ratio as a jet gas. Since helium is a very light gas, R_j was varied over a wide range by changing the mixing ratio. As a result, a large value of the RT product could be obtained without elevating gas temperature.

Figure 15 shows the effect of mole fraction of helium in a nitrogen-based jet gas on base pressure. It can be seen that C_{pb} increases with increasing mole ratio of He (increasing R_j). This trend is similar to that of the jet-temperature variation shown in Fig. 5.

In Fig. 16, the same data in Figs. 5 and 15 are plotted as a function of the d_1/d_e and the mass flow ratio. Open symbols indicate the data obtained for a N_2 jet in the 0.1-m TCWT test, in which T_{tj} is variable

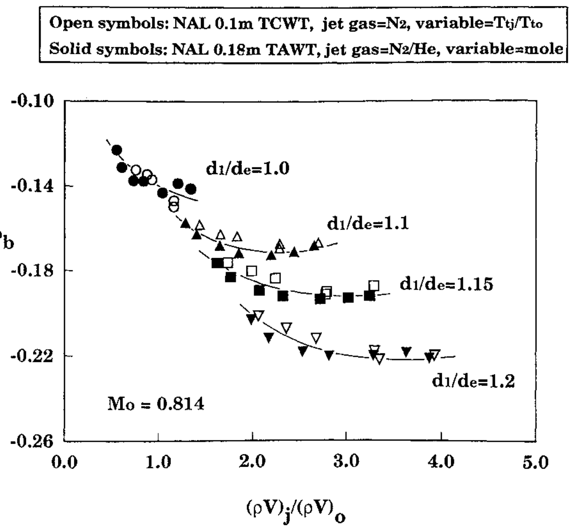

Fig. 16 Simulation of jet temperature effects using low-molecular-weight cold gas.

whereas R_j and γ_j are constant. On the other hand, solid symbols indicate the data from the 0.18-m TAWT test, in which R_j and γ_j are variable, whereas T_{tj} is held constant (ambient). As clearly seen in Fig. 16, the data obtained in the two tunnels are practically the same. This result indicates that the effect of jet temperature on base flow can be simulated in an ambient wind tunnel using a cold gas having low molecular weight.

In Ref. 4, Peters proposed a correction method for the jet temperature effect on transonic afterbody drag. He suggested using mass flux ratio as a possible correlation parameter for entrainment effect. The previous conclusion supports the validity of Peters' suggestion. It is noted here that Peters' work was conducted on typical airplane-type boat-tail nozzles. It is known that, for an afterbody nozzle with high boat-tail angle (25 deg, for example), flow separation occurs at the nozzle aft end. This is similar to the blunt-based flow studied in this report. Although further studies will be needed to fully understand the underlying flow mechanism, it is expected that the similarity rule derived from this study should work for other afterbody configurations.

Conclusions

By using a cryogenic approach, the effects of jet temperature on the transonic base pressure of a cylindrical blunt-based afterbody model have been investigated. Analyzing the data obtained for various jet conditions, a number of conclusions were drawn concerning the similarity rule for jet-temperature effects on the transonic base pressure;

1) The base pressure, for constant *NPR* and γ_j, is a function of the product of gas constant and jet temperature. This indicates that the jet entrainment effect is related to the product *RT* of a jet. The inference previously made by Peters has been confirmed.

2) The base pressure data obtained for various jet conditions can be correlated very well with two parameters: one is the plume maximum diameter d_1/d_e for the plume shape effect, and the other is the mass flux ratio $(\rho V)_j/(\rho V)_0$ for the jet entrainment effect.

3) The net effect of jet-temperature elevation is an increase in the base pressure (reduction in the base drag). This result agrees with the previous flight experiences of the Tornado and Space Shuttle vehicles.

4) Utilizing a similarity rule derived from the cryogenic experiment, the effects of jet temperature on the base pressure can be simulated in an ambient wind tunnel with a cold jet gas having low molecular weight.

5) As has been demonstrated in the present study, the cryogenic approach can provide an excellent tool for fundamental similarity research on jet temperature effects.

Acknowledgments

The author would like to acknowledge Hideo Sawada and Takeo Aoki for their assistance in conducting tests in the NAL 0.1-m TCWT. The author also thanks Asao Hanzawa and Yoshimi Iijima for their help in conducting tests in the NAL 0.18-m TAWT.

References

[1] Carter, E. C., "Jet-Temperature Effects," *Aerodynamics of Aircraft Afterbody*, AGARD AR-226, June 1986, Sec. 3.2.1., pp. 233–244.

[2] Roberts, B. B., Wallace, R. O., and Sims, J. L., "Plume Base Flow Simulation Technology," *Shuttle Performance: Lessons Learned*, NASA CP 2283, Pt. 1, March 1983.

[3] Compton, W. B., III, "Effects of Jet Exhaust Gas Properties on Exhaust Simulation and Afterbody Drag," NASA TR R-444, 1975.

[4] Peters, W. L., "A Simulation Technique for Jet Temperature Effects on Nozzle-Afterbody Drag at Transonic Mach Numbers," AIAA Paper 85-1463, July 1985.

[5] Peters, W. L., "A Comparison of Jet Temperature Effects on Afterbody Drag with Those from Jet Molecular Weight and Nozzle Area Ratio Variations," AIAA Paper 80-1161, June 1980.

[6] Asai, K., "Hot-Jet Simulation in Cryogenic Wind Tunnels," NASA RP-1220, July 1989.

[7] Asai, K., and Aoki, T., "Experiments to Evaluate Hot-Jet Simulation Capabilities in Cryogenic Wind-Tunnel Testing," AIAA Paper 92-0567, Jan. 1992.

[8] Asai, K., "The Cryogenic Approach to Simulating Hot Jet in Transonic Wind-Tunnel Testing," 18th Congress of the International Council of the Aeronautical Sciences, Paper 92-3.6.1, Beijing, PRC, Sept. 1992.

[9] Takashima, K., Sawada, H., Aoki, T., and Kayaba, S., "Trial Manufacture of NAL 0.1 m × 0.1 m Transonic Cryogenic Wind Tunnel," National Aerospace Lab., NAL TR-910, Tokyo, Japan, Aug. 1986 (in Japanese).

[10] Hashimoto, N., and Inoue, S., "Operational Tests of the NAL 0.18 m Transonic Wind Tunnel," National Aerospace Lab., NAL TM-6, Tokyo, Japan, Aug. 1962 (in Japanese).

[11] Merz, R. A., Page, R. H., and Przirembel, C. E. G., "Subsonic Axisymmetric Near-Wake Studies," *AIAA Journal*, Vol. 16, No. 7, 1978, pp. 656–662.